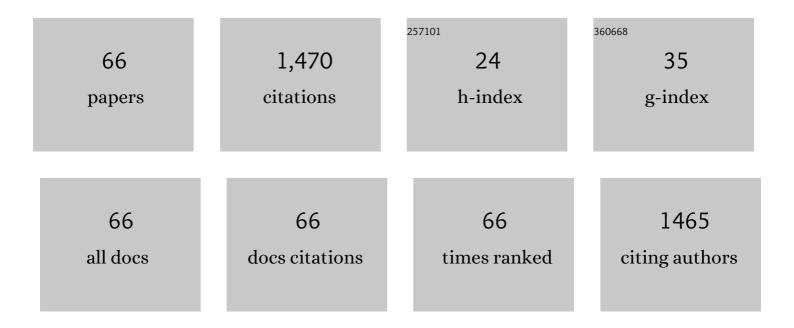
List of Publications by Year in descending order

Source: https://exaly.com/author-pdf/9079368/publications.pdf Version: 2024-02-01



#	Article	IF	CITATIONS
1	Evaporation rate far beyond the input solar energy limit enabled by introducing convective flow. Chemical Engineering Journal, 2022, 429, 132335.	6.6	31
2	Designing hard, low-refractive-index lossy materials for super wear-resistant absorbers. Materials Research Letters, 2022, 10, 472-480.	4.1	2
3	3D Hydrogel Evaporator with Vertical Radiant Vessels Breaking the Tradeâ€Off between Thermal Localization and Salt Resistance for Solar Desalination of Highâ€Salinity. Advanced Materials, 2022, 34, .	11.1	73
4	Designing infrared phase change materials for colorful infrared transmittance modulators. Applied Surface Science, 2022, 600, 154104.	3.1	1
5	Three distinct optical-switching states in phase-change materials containing impurities: From physical origin to material design. Journal of Materials Science and Technology, 2021, 75, 118-125.	5.6	9
6	Biomass-Derived Carbonaceous Materials with Multichannel Waterways for Solar-Driven Clean Water and Thermoelectric Power Generation. ACS Sustainable Chemistry and Engineering, 2021, 9, 4571-4582.	3.2	56
7	Integration of superhydrophobicity and high durability in super-rough hard thin films. Ceramics International, 2021, 47, 23653-23658.	2.3	7
8	Full-color, multi-level transmittance modulators: From reflectivity/gradient absorption coupling mechanism to materials map. Acta Materialia, 2021, 216, 117132.	3.8	2
9	Towards highly efficient solar-driven interfacial evaporation for desalination. Journal of Materials Chemistry A, 2020, 8, 17907-17937.	5.2	115
10	Phase Change Materials for Nonvolatile, Solidâ€State Reflective Displays: From New Structural Design Rules to Enhanced Colorâ€Changing Performance. Advanced Optical Materials, 2020, 8, 2000062.	3.6	12
11	"All-crystalline―phase transition in nonmetal doped germanium–antimony–tellurium films for high-temperature non-volatile photonic applications. Acta Materialia, 2020, 188, 121-130.	3.8	17
12	<i>In situ</i> growth of ultra-smooth or super-rough thin films by suppression of vertical or horizontal growth of surface mounds. Journal of Materials Chemistry C, 2020, 8, 3248-3257.	2.7	7
13	Improving the reflectance and color contrasts of phase-change materials by vacancy reduction for optical-storage and display applications. Optics Letters, 2020, 45, 244.	1.7	5
14	Optical coatings of durability based on transition metal nitrides. Thin Solid Films, 2019, 688, 137339.	0.8	27
15	The role of structural order and stiffness in the simultaneous enhancement of optical contrast and thermal stability in phase change materials. Journal of Materials Chemistry C, 2019, 7, 4132-4142.	2.7	13
16	Novel SPR sensing platform based on superstructure MoS2 nanosheets for ultrasensitive detection of mercury ion. Sensors and Actuators B: Chemical, 2019, 284, 589-594.	4.0	47
17	Understanding phase-change materials with unexpectedly low resistance drift for phase-change memories. Journal of Materials Chemistry C, 2018, 6, 3387-3394.	2.7	20
18	New design for highly durable infrared-reflective coatings. Light: Science and Applications, 2018, 7, 17175-17175.	7.7	37

#	Article	IF	CITATIONS
19	Tribochemistry dependent tribological behavior of superhard TaC/SiC multilayer films. Surface and Coatings Technology, 2018, 337, 492-500.	2.2	29
20	Structural evolution and dielectric properties of Nd and Mn co-doped BaTiO 3 ceramics. Journal of Alloys and Compounds, 2018, 760, 31-41.	2.8	43
21	Surface roughening transition induced by phase transformation in hafnium nitride films. Surface and Coatings Technology, 2017, 320, 414-420.	2.2	3
22	Improving electrical conductivity and wear resistance of hafnium nitride films via tantalum incorporation. Ceramics International, 2017, 43, 8517-8524.	2.3	12
23	Combined effect of ion bombardment and nitrogen incorporation on structure, mechanical and optical properties of amorphous Ge2Sb2Te5 films. Vacuum, 2017, 141, 32-40.	1.6	2
24	Oxygen vacancies dependent phase transition of Y2O3 films. Applied Surface Science, 2017, 410, 470-478.	3.1	31
25	Improved multi-level data storage properties of germanium-antimony-tellurium films by nitrogen doping. Scripta Materialia, 2017, 141, 120-124.	2.6	21
26	Highly hard yet toughened bcc-W coating by doping unexpectedly low B content. Scientific Reports, 2017, 7, 9353.	1.6	15
27	N dependent tribochemistry: Achieving superhard wear-resistant low-friction TaC x N y films. Surface and Coatings Technology, 2017, 328, 378-389.	2.2	23
28	Optical reflectivity and hardness improvement of hafnium nitride films via tantalum alloying. Applied Physics Letters, 2016, 109, 232102.	1.5	8
29	Ion-bombardment-induced reduction in vacancies and its enhanced effect on conductivity and reflectivity in hafnium nitride films. Applied Physics A: Materials Science and Processing, 2016, 122, 1.	1.1	3
30	Structural evolution and optical properties of hydrogenated germanium carbonitride films. Vacuum, 2016, 129, 23-30.	1.6	2
31	Transformation of electronic properties and structural phase transition from HfN to Hf ₃ N ₄ . Journal of Physics Condensed Matter, 2015, 27, 225501.	0.7	7
32	Identification and thermodynamic mechanism of the phase transition in hafnium nitride films. Acta Materialia, 2015, 90, 59-68.	3.8	31
33	Hardness and optical gap enhancement of germanium carbon films by nitrogen incorporation. Thin Solid Films, 2015, 584, 208-213.	0.8	5
34	Negative effect of vacancies on cubic symmetry, hardness and conductivity in hafnium nitride films. Scripta Materialia, 2015, 108, 141-146.	2.6	25
35	Structure, mechanical and tribological properties of HfCx films deposited by reactive magnetron sputtering. Applied Surface Science, 2015, 327, 68-76.	3.1	30
36	Nature of Tunable Optical Reflectivity of Rocksalt Hafnium Nitride Films. Journal of Physical Chemistry C, 2014, 118, 20511-20520.	1.5	23

#	Article	IF	CITATIONS
37	On the nature of point defect and its effect on electronic structure of rocksalt hafnium nitride films. Acta Materialia, 2014, 81, 315-325.	3.8	31
38	The AlN layer thickness dependent coherent epitaxial growth, stress and hardness in NbN/AlN nanostructured multilayer films. Surface and Coatings Technology, 2013, 235, 367-375.	2.2	24
39	Relationship between dielectric coefficient and Urbach tail width of hydrogenated amorphous germanium carbon alloy films. Applied Physics Letters, 2012, 101, 042109.	1.5	10
40	Effects of substrate bias voltage on the microstructure, mechanical properties and tribological behavior of reactive sputtered niobium carbide films. Surface and Coatings Technology, 2012, 212, 185-191.	2.2	47
41	Field emission properties of vertically aligned thin-graphite sheets/graphite-encapsulated Cu particles. Applied Surface Science, 2012, 258, 6930-6937.	3.1	9
42	Influence of the residual stress on the nanoindentation-evaluated hardness for zirconiumnitride films. Surface and Coatings Technology, 2012, 206, 3250-3257.	2.2	31
43	Structure, mechanical property, and tribological behavior of c-NbN/CNx multilayers grown by magnetron sputtering. Surface and Coatings Technology, 2012, 206, 4040-4045.	2.2	18
44	Modulation periodicity dependent structure, stress, and hardness in NbN/W2N nanostructured multilayer films. Journal of Applied Physics, 2011, 109, .	1.1	12
45	Role of carbon in the formation of hard Ge1â^'xCx thin films by reactive magnetron sputtering. Physica B: Condensed Matter, 2011, 406, 2658-2662.	1.3	12
46	Preferred orientation, phase transition and hardness for sputtered zirconium nitride films grown at different substrate biases. Surface and Coatings Technology, 2011, 205, 2865-2870.	2.2	42
47	Ar plasma treatment on few layer graphene sheets for enhancing their field emission properties. Journal Physics D: Applied Physics, 2010, 43, 055302.	1.3	69
48	Increasing sp3hybridized carbon atoms in germanium carbide films by increasing the argon ion energy and germanium content. Journal Physics D: Applied Physics, 2010, 43, 135103.	1.3	18
49	Effects of bonding structure from niobium carbide buffer layer on the field electric emission properties of a-C films. Journal of Applied Physics, 2009, 105, 074318.	1.1	1
50	Relatively low temperature synthesis of hexagonal tungsten carbide films by N doping and its effect on the preferred orientation, phase transition, and mechanical properties. Journal of Vacuum Science and Technology A: Vacuum, Surfaces and Films, 2009, 27, 167-173.	0.9	19
51	Field electron emission enhancement of amorphous carbon through a niobium carbide buffer layer. Journal of Applied Physics, 2009, 105, .	1.1	2
52	Effects of nitrogen flow rate on the preferred orientation and phase transition for niobium nitride films grown by direct current reactive magnetron sputtering. Journal Physics D: Applied Physics, 2009, 42, 035304.	1.3	27
53	Annealing effects on the bonding structures, optical and mechanical properties for radio frequency reactive sputtered germanium carbide films. Applied Surface Science, 2009, 255, 3552-3557.	3.1	26
54	Stress induced preferred orientation and phase transition for ternary WCxNy thin films. Applied Surface Science, 2009, 255, 8164-8170.	3.1	7

#	Article	IF	CITATIONS
55	Structure and mechanical properties of δ-NbN/SiNx and δ′-NbN/SiNx nano-multilayer films deposited by reactive magnetron sputtering. Surface and Coatings Technology, 2009, 203, 1702-1708.	2.2	28
56	Effects of bias voltage and annealing on the structure and mechanical properties of WC0.75N0.25 thin films. Journal of Alloys and Compounds, 2009, 486, 357-364.	2.8	20
57	Structures, mechanical properties and thermal stability of TiN/SiNx multilayer coatings deposited by magnetron sputtering. Journal of Alloys and Compounds, 2009, 486, 515-520.	2.8	28
58	Multilayer antireflective and protective coatings comprising amorphous diamond and amorphous hydrogenated germanium carbide for ZnS optical elements. Thin Solid Films, 2008, 516, 3117-3122.	0.8	22
59	Interfacial fracture for TiN/SiNx nano-multilayer coatings on Si(111) characterized by nanoindentation experiments. Materials Science & amp; Engineering A: Structural Materials: Properties, Microstructure and Processing, 2008, 494, 324-328.	2.6	18
60	Effects of substrate bias on the preferred orientation, phase transition and mechanical properties for NbN films grown by direct current reactive magnetron sputtering. Journal of Applied Physics, 2008, 104, .	1.1	43
61	Field electron emission enhancement of amorphous carbon through a niobium buffer layer. Journal of Applied Physics, 2008, 103, 114314.	1.1	4
62	Effects of radio frequency power on the chemical bonding, optical and mechanical properties for radio frequency reactive sputtered germanium carbide films. Journal Physics D: Applied Physics, 2006, 39, 5074-5079.	1.3	17
63	Effects of the chemical bonding on the optical and mechanical properties for germanium carbide films used as antireflection and protection coating of ZnS windows. Journal of Physics Condensed Matter, 2006, 18, 4231-4241.	0.7	31
64	Ge1–xCx double-layer antireflection and protection coatings. Applied Surface Science, 2006, 252, 8135-8138.	3.1	22
65	Chemical bonding of a-Ge1â [•] xCx:H films grown by RF reactive sputtering. Vacuum, 2004, 77, 63-68.	1.6	20
66	Thermal stability of magnetron sputtering amorphous carbon nitride films. Vacuum, 2003, 72, 233-239.	1.6	18